Computational Fluid Dynamics Analysis of Two-Phase Thermosyphon

Nikhil E. Chaudhari #1, Nishtha Vijra #2, T. P. Singh #3
Symbiosis International University, Pune, Maharashtra, India
[1] nikhilchaudhari245@yahoo.in
[2] nishthav@sitpune.edu.in
[3] director@sitpune.edu.in

***Abstract*— Computational fluid dynamics (CFD) analysis of two phase thermosyphon has been considered in the present study, under steady state conditions using ANSYS-CFX software. In wickless heat pipe or a thermosyphon, latent heat of vaporization and latent heat of condensation are mainly responsible for very high rate of heat transfer. CFD analysis was carried out to predict the overall temperature distribution. CFD results were used to calculate the effective overall thermal resistance of thermosyphon for three different heat inputs. The overall thermal resistance was found to decrease with increase in heat input. The CFD predicted temperatures at various sections of thermosyphon were found to be in good agreement with the experimental results.**

Keyword-Two-phase thermosyphon, CFD

I. INTRODUCTION

Thermosyphon is a heat transfer device capable of high heat transfer with small temperature gradient over the large distance. It is an enclosed sealed tube used to transfer heat from heat source to the heat sink using latent heat of evaporation and latent heat of condensation of the working fluid present in the thermosyphon. The thermosyphon mainly consists of evaporator section, adiabatic section and condenser section. It is also called as wickless heat pipe due to absence of wick and instead uses the gravity effect for the transportation of the condensed fluid to the evaporator region, hence it is normally kept in inclined or vertical position, with condenser section above the evaporator section. The main purpose for using thermosyphon is that it can provide very high thermal conductance even higher than the best available metallic conductor, and is more effective in heat transfer compared to the solid conductor of same cross-sectional area. Fig.1 shows the schematic diagram of thermosyphon.

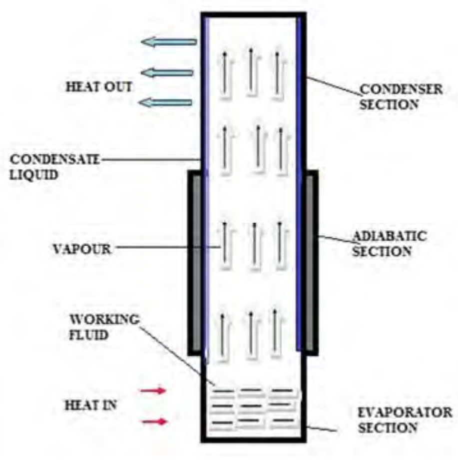

Fig.1. Schematic diagram of thermosyphon

The heat is added to the evaporator section and as a result the working fluid present in the thermosyphon gets heated and gets converted to vapour with latent heat of vaporization. Due to density differences, the vapour moves to the top towards condenser section thereby rejecting heat and thus gets converted to liquid form and returns back to the evaporator section due to gravitational effect. The cycle thus continues till the application of heat. The advantages of thermosyphon are that it is compact, has no moving parts, makes no noise, is free of vibrations and is also robust. The main applications of thermosyphon system are in solar applications, waste heat recovery systems, air conditioning systems, electrical and electronics systems.

Many researchers have performed extensive experimentation and numerical analysis on thermosyphon to study the thermal characteristics and performance of the thermosyphon system. Payakaruk et al. [2] studied the effect of filling ratio and working fluid on the heat transfer rate at various inclined positions of thermosyphon.

Monde and Mitsutake [3] carried the experimentation to enhance the critical heat flux using a concentric tube connected between the heated chamber and upper cooling chamber. Kiatsiriroat [4] studied the thermal performance of thermosyphon using binary working fluids as ethanol-water and triethylene glycol (TEG)-water. It was found that at low temperature ethanol-water had higher heat transfer than water while, for TEG-water mixture heat transfer rate increased with increase of TEG content in mixture. Park and Kang [5] investigated the heat transfer characteristics for the varying fill ratio in two phase close thermosyphon.It was found that the heat transfer coefficient of evaporator had negligible effect, while heat transfer coefficient of condenser showed some enhancement with increase of fill charge ratio. Khodabandeh [6] studied the thermal performance of a thermosyphon for cooling of radio base stations at operating conditions. Baudouy [7] determined the critical heat flux as a function of the heated length of the tube and also presented the boiling curves with a detailed analysis of hysteresis effect on temperature excursion was performed. Nada et al. [8] studied the performance of a two phased closed thermosyphon solar collector with a shell and tube heat exchanger. The study showed that number of tubes had a significant effect on the collector efficiency. The performance of thermosyphon solar collector obtained was better than shell and tube heat exchanger. Zhang et al. [9] studied the thermal performance characteristics of transparent two phase thermosyphon. The experimental results showed that the thermosyphon with the grooved evaporation surface had much better performance than the smooth surface. Yang and Chang [10] conducted experimentation on reciprocating tilted thermosyphon. A set of empirical heat transfer correlations permitting the evaluation of axially averaged Nusselt number was developed. Jouhara and Robinson [11] used the working fluid as Therminol VP1 and Dowtherm A for operating range of 200 C to 450 C.The study showed that up to 420 C, very high effective thermal conductivity (20 kW/m-K) and very low thermal resistance (0.4K/W) was obtained with both the working fluid. Vijra and Singh [12] studied the application of the thermosyphon system in process industry. An alternative method using thermosyphon was proposed for the efficient and economic cooling of mechanical seals instead of the prevalent water jacketing method. Gandikota et al. [13] conducted experiments using carbon fiber epoxy heat sink for evaporator surface enhancement. Rahimi et al. [14] studied the effect of the condenser and evaporator resurfacing on overall performance of the thermosyphon. It was found that making the evaporator more hydrophilic and condenser more hydrophobic, the thermal performance increased and thermal resistance decreased in comparison to conventional thermosyphon. Tsai et al. [15] studied the application of the two phase closed thermosyphon in the electronic cooling to enhance the heat transfer rate. Jouhara and Robinson [16] made a comparison on the basis of the performance of the thermosyphon using working fluid as water, FC -84, FC-77 and FC-3283. It was observed that water charged thermosyphon performed better than the other three working fluids for the effective thermal resistance and for maximum heat transfer. In this study experimentation was performed by applying different levels of heat inputs to thermosyphon. Ong [17] conducted experimental investigations to determine the thermal performance of R-134a filled thermosyphon heat exchanger and water filled heat pipe heat exchanger. Overall effectiveness ranged from 0.8 to 0.5 for thermosyphon heat exchanger and from 0.9 to 0.3 for heat pipe heat exchanger. Huminic et al. [18] and Yang and Liu [21] performed experimental investigations on use of solid nano particles added to water as a working fluid. Edge et al. [19] studied the one dimensional process model for steam generation in a natural circulation boiler linked to a detailed 3D CFD model of the coal fired furnaces. The CFD model was validated with typical data from the 500MW subcritical power plant. Annamalai and Ramalingam [20] carried the CFD analysis of air cooled condenser heat pipe. The CFD results were compared with the results obtained experimentally.

Literature review shows that most of the analysis was carried out experimentally. CFD being recent and powerful tool can be used to analyse the temperature distribution of thermosyphon. In this study, steady CFD analysis of thermosyphon has been conducted to obtain the temperature distribution on the surface of the thermosyphon applying the temperatures obtained experimentally for three levels of heat inputs to the evaporator section. The basic CFD procedure was followed and multi- phase steady state analysis was performed. CFD result was also used to calculate overall effective thermal resistance of thermosyphon.

II. CFD PROCEDURE

In the present study basic CFD steps were carried out to perform multi-phase analysis with the help of ANSYS 13 software. CFX solver was used for problem setup and analysis. Results were viewed in CFD post. Fig.2. shows the basic steps followed in CFD for solving the problem.

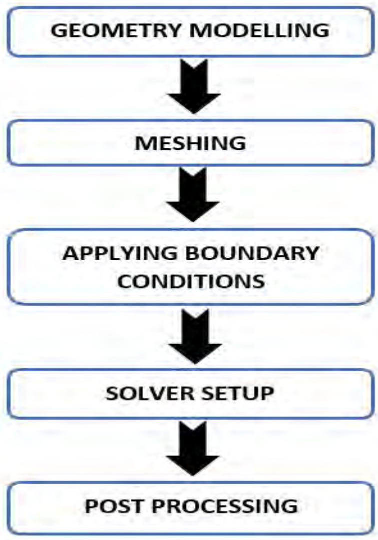

Fig.2. Basic steps solved in CFD

III. GEOMETRIC MODELLING

3-D Fluid domain was modelled in ANSYS Workbench. The thermosyphon inner and outer diameters were 6mm and 12mm respectively. The total length of thermosyphon pipe was 200mm with 40mm evaporator section, 60mm condenser section and rest 100mm as adiabatic section [16]. The vertical position of thermosyphon was considered with condenser section above the evaporator section. Meshing was done to discretise the fluid domain. Discretising changed the differential form of governing equations to a system of algebraic equations. In the present study hexahedral elements were used for meshing. About 11128 element and 13545 nodes were formed during meshing. Fig.3 shows geometry of the thermosyphon and Fig.4 shows the meshed model. The elements formed were in agreement with the quality criteria. Table I shows the mesh statistics.

TABLE I
Details of Meshing

Mesh Metric	Minimum Value	Maximum Value	Average Value
Aspect Ratio	1.2588	2.1165	1.508
Skewness	0.02677	0.3593	0.1926
Warping Factor	0.0000012	0.000055	0.0000145
Jacobian Ratio	1.022	2.591	1.510

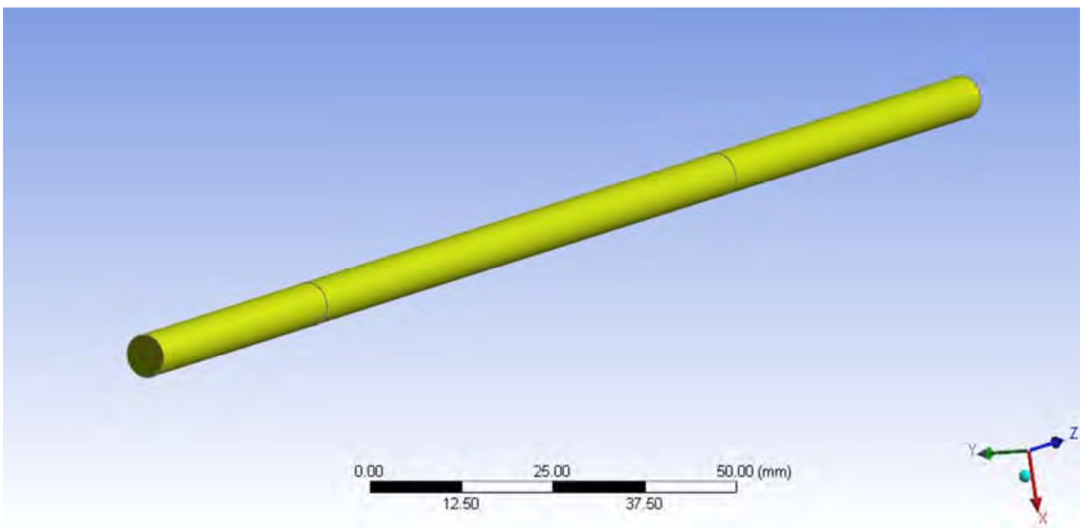

Fig.3. Geometry modelling of thermosyphon in ANSYS Workbench

IV. BOUNDARY CONDITIONS

The setup was formed in CFX software where boundary conditions were applied. Water as ideal gas and water was considered in fluid domain with appropriate volume fraction. The fixed temperature boundary condition was applied at the evaporator end. No slip wall condition and adiabatic boundary condition was applied in the adiabatic section. Heat transfer coefficient and ambient temperature boundary condition were applied to condenser wall with no slip condition. The buoyancy force was activated with acceleration due to gravity as 9.81 m/sec^2 in negative Z direction. The boundary conditions for evaporator wall, adiabatic wall and condenser wall are given in Table II

TABLE II
Boundary Conditions

Evaporator Wall	Adiabatic Wall	Condenser Wall
$T = T_w$	$\frac{\partial q}{\partial r} = 0$	$\frac{\partial q}{\partial r} = h(T_w - T_a)$
U=V=W=0	*U=V=W=0*	*U=V=W=0*

Where T_w is the wall temperature, T_a is the ambient temperature, r is outer radius, q is the heat transfer, h is the heat transfer coefficient. U, V and W are the velocity components in x, y and z direction respectively.

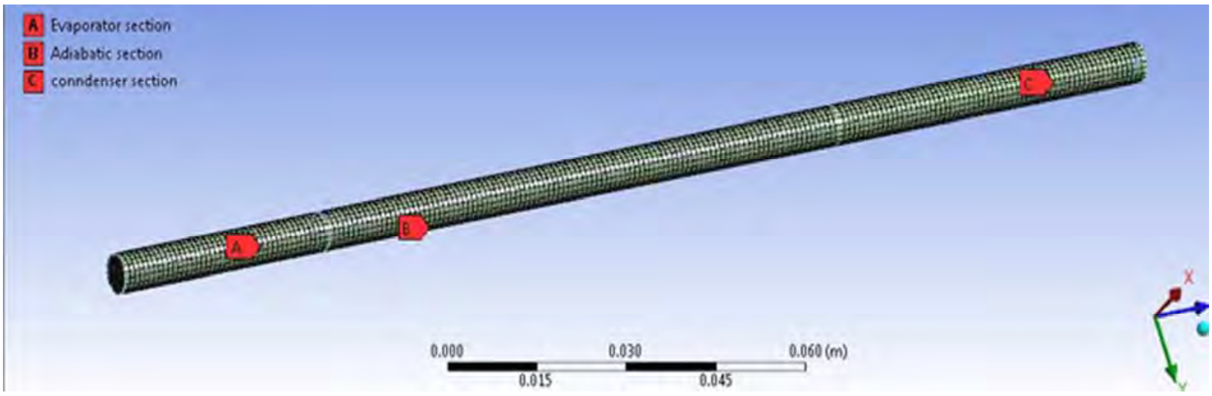

Fig.4. Meshed Thermosyphon

V. SOLVER PARAMETER

High resolution advection scheme was used with root mean square (RMS) residual type set as convergence criteria. The RMS target 1e-4 was set to obtain converged solution. Minimum of one iteration and maximum of three thousand iterations were set to obtain the solution. Auto timescale was set for fluid timescale control and length scale option was set up conservative to run the setup.

VI. RESULTS AND DISCUSSION

The problem setup formed was solved in CFX solver and about three thousand iterations were carried to obtain required converge solution. The contour diagram obtained for temperature profile of thermosyphon wall for heat input of 100 W, 120.5 W and 180W are shown in Fig.5, Fig.6 and Fig.7 respectively. The evaporator section had a high temperature due to application of heat in this section. The temperature in adiabatic section almost remained constant. The condenser section showed gradual decrease of temperature due to heat rejection to surrounding. Maximum temperature was obtained as 364.4 K and minimum temperature of 327.5 K was obtained. In CFD analysis the adiabatic section showed same range of temperature as in evaporator section, due to no heat loss through adiabatic section. Almost similar contours were obtained for heat inputs of 120.5 watts and 180watts with higher temperatures.

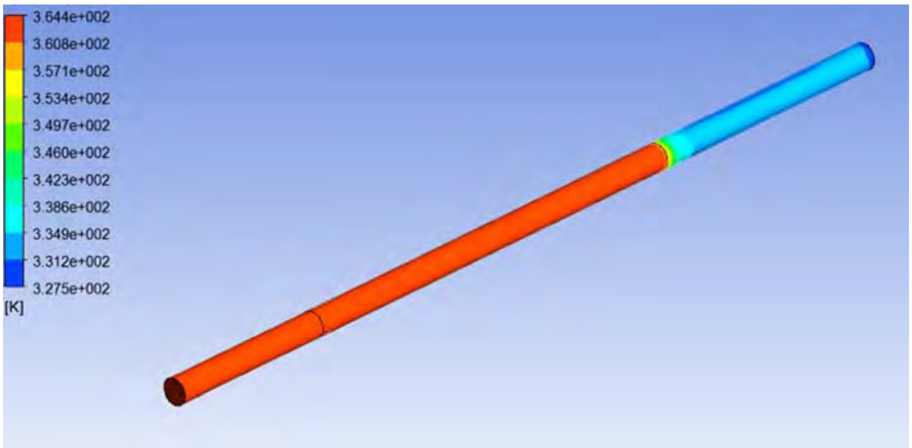

Fig.5. Contour diagram for heat input of 100 W

With increase in heat input the temperatures of the evaporator section, adiabatic section and condenser section were also found to increase, although the temperature decreased axially from the evaporator section to the condenser section. In addition to this, the increase in the surface temperature of the evaporator section was found to be more significant with increase in heat input than the adiabatic and condenser surface temperatures.

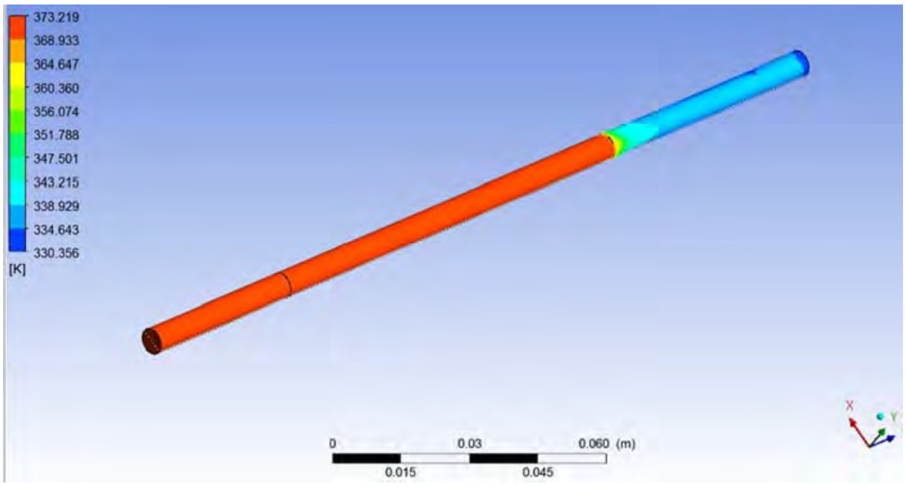

Fig.6. Contour diagram for heat input of 120.5 W

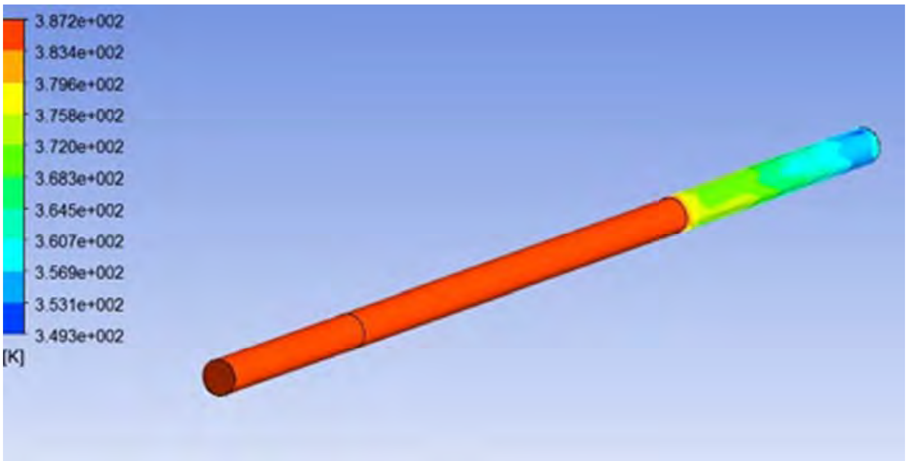

Fig.7 Contour diagram for heat input of 180 W

Jouhara et al. [16] carried experimentation to obtain temperature profile on the surface along the length of thermosyphon pipe for different heat inputs including for 100W, 120.5W and 180W. These experimental results were the basis to validate the CFD results obtained from present study. The comparison of CFD results and experimentation results for three different heat inputs are shown in Fig.8, Fig.9 and Fig.10 for heat input of 100W, 120.5W and 180W respectively.

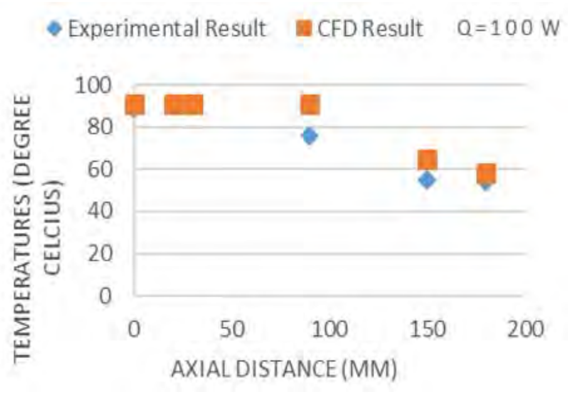

Fig.8 Comparison of Experimental Results [16] and CFD Results

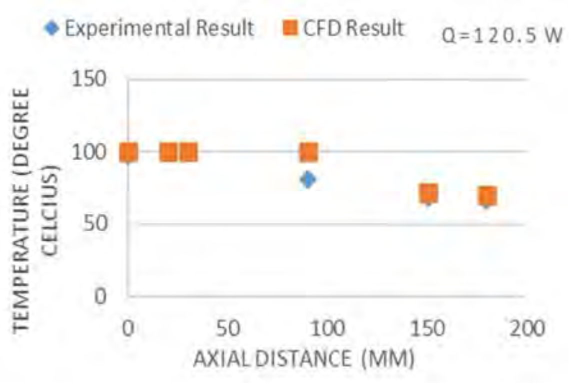

Fig.9. Comparison of Experimental Results [16] and CFD Results

Figure 8 shows the comparison of temperature obtained by experimentation and computational fluid dynamics analysis for 100 W input. Good agreement was seen between CFD results and experimental values except for the deviation seen in adiabatic section. Practically there is always some heat loss through adiabatic section. In CFD software ideal adiabatic condition was considered and so the deviation was obtained while comparing both the results. Maximum deviation of 11% was seen in condenser section due to different ambient condition considered. Almost similar trends were obtained for heat input of 120.5 W and 180W.

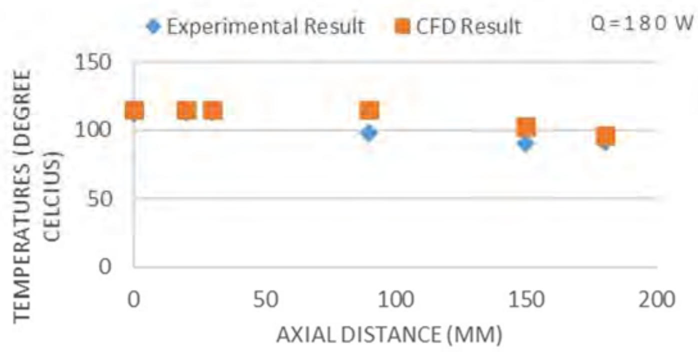

Fig.10. Comparison of Experimental Results [16] and CFD Results

Electrical analogue form [16] was applied for calculating the effective overall thermal resistance using the acquired CFD results with the help of following equation.

$$R_o = T_e - T_c / Q \tag{1}$$

Where R_o is effective overall thermal resistance of thermosyphon, T_e and T_c are the average evaporator and condenser wall temperature respectively. It was observed that with increase in heat input, the effective overall thermal resistance decreased.

TABLE III
Overall Thermal Resistance

Heat input	**R_o (K/W)**
100 watt	0.295
120.5 watt	0.24
180 watt	0.0861

Table III shows the effective overall thermal resistance for three levels of heat inputs calculated using equation 1.The possible reason of low overall effective thermal resistance with increase in heat input/power input is due to the enhancement of boiling techniques. The nucleate boiling activity improves in the evaporator section with increase in power input there by reducing the thermal resistance of the evaporator section hence reducing the overall effective thermal resistance of the thermosyphon.

VII. CONCLUSION

Computational fluid dynamics is a powerful tool to model and analyze the thermosyphon to predict the surface temperature distribution. Computational fluid dynamics two phase analysis was performed and temperature profile obtained was in fair agreement with the experimental results. The over prediction of temperature found from CFD analysis in adiabatic section was also noted and hence a deviation from the experimental results was found. It was found that rise in surface temperature of evaporator section was more noteworthy with increase in heat input compared to adiabatic and condenser section. The effective overall thermal resistance for heat input of 180 watt was found to be lowest than the heat input of 100 watt and 120.5 watt. The improvement in boiling activity with increase in heat input enhanced the performance of thermosyphon. Thermosyphon with higher heat input was more effective in heat transfer compared to lower range of heat input.

REFERENCES

[1] J. D. Anderson. Jr, *Computational Fluid Dynamics: The Basics with Applications*, McGraw-Hill International Editions, 1995

[2] T. Payakaruk, P. Terdtoon, S. Ritthidech. "Correlations to predict heat transfer characteristics of an inclined closed two-phase thermosyphon at normal operating conditions," Applied Thermal Engineering, vol. 20, pp.781-790, 2000.

[3] M. Monde and Y. Mitsutake, "Enhancement of CHF in open thermosyphon with heated bottom chamber," International Journal of Heat and Mass Transfer, vol. 43, pp. 3341-3346, 2000.

[4] T. Kiatsiriroat, "Thermal Performance Enhancement of Thermosyphon Heat Pipe with Binary Working Fluids," Experimental Heat Transfer, vol. 13, pp.137-152, 2000.

[5] J. Park, Hwan Kook Kang, Chul Ju Kim, "Heat transfer characteristics of a two-phase closed thermosyphon to the fill charge ratio," International journal of heat and mass transfer, vol. 45, pp. 4655-4661, 2002.

[6] R. Khodabandeh , "Thermal performance of a closed advanced two-phase thermosyphon loop for cooling of radio base stations at different operating conditions," Applied Thermal Engineering, vol. 24, pp. 2643-2655, 2004.

[7] B. Baudouy, "Heat Transfer near Critical Condition Intwo-Phase He I Thermosiphon Flow Atlow Vapor Quality," Cryogenic Engineering conference, vol. 49, pp. 0-7354-0186-1, 2004.

[8] S.A. Nada , H.H. El-Ghetany, H.M.S. Hussein, "Performance of a two-phase closed thermosyphon solar collector with a shell and tube heat exchanger," Applied Thermal Engineering, vol. 24, pp. 1959-1968, 2004.

[9] M. Zhang, Z. Liu, G. Ma, "The experimental investigation on thermal performance of a flat two-phase thermosyphon," International Journal of Thermal Sciences, vol. 47, pp.1195-1203, 2008.

[10] T. L.Yang and S. W. Chang, "Heat transfer in tilted reciprocating anti-gravity open thermosyphon," International journal of heat and mass transfer, vol. 52, pp. 880-893, 2009.

[11] H. Jouhara and A. J. Robinson, "An Experimental Study of Small-Diameter Wickless Heat Pipes Operating in the Temperature Range 200◦C to 450◦C", Heat Transfer Engineering, vol. 30, pp. 1041-1048, 2009.

[12] N. Vijra and T. P. Singh, "Enhanced Air Finned Cooler to improve the sustainability and life of Mechanical Seals", International Journal of Earth Science and Engineering, ISSN 0974-5904, 2009.

[13] V. Gandikota, G. F. Jones, A. S. Fleischer, "Thermal performance of a carbon fiber composite material heat sink in an FC-72 thermosyphon", Experimental Thermal and Fluid Science, vol. 34, pp. 554-561, 2010.

[14] M. Rahimi, K. Asgary, S.Jesri, "Thermal characteristics of a resurfaced condenser and evaporator closed two-phase thermosyphon", International Communications in Heat and Mass Transfer, vol. 37, pp. 703-710, 2010.

[15] T.Tsai, Wu, C. Chang, S. Chen, "Two-phase closed thermosyphon vapor-chamber system for electronic cooling", International Communications in heat and mass Transfer, vol. 37, pp. 484-489, 2010.

[16] H. Jouhara and A. J. Robinson, "Experimental investigation of small diameter two-phase closed thermosyphons charged with water, FC-84, FC-77 and FC-3283", Applied Thermal Engineering, vol. 30, pp. 201-211, 2010.

[17] K. S. ONG, "Experimental Performance of R-134a-Filled and Water-Filled Loop Heat Pipe Heat Exchangers", Heat transfer Engineering, vol. 31, pp. 1091-1097, 2010.

[18] G. Huminic, A. Huminic, I. Morjan, F. Dumitrache, "Experimental study of the thermal performance of thermosyphon heat pipe using iron oxide nano particles", International Journal of Heat and Mass Transfer, vol. 54, pp. 656-661, 2011.

[19] A. S. Annamalai and V. Ramalingam, "Experimental Investigation and Computational Fluid Dynamics Analysis of an Air Cooled Condenser Heat Pipe", Thermal Science, vol. 15, pp. 759-772, 2011.

[20] P.J. Edge, P.J. Heggs, M. Pourkashanian, A. Williams, "An integrated computational fluid dynamics–process model of natural circulation steam generation in a coal-fired power plant", Computers and Chemical Engineering, vol. 35, pp. 2618-2631, 2011.

[21] X. Yang and Z. Liu, "Flow boiling heat transfer in the evaporator of a loop thermosyphon operating with CuO based aqueous nanofluid", International Journal of Heat and Mass Transfer, vol. 55, pp.7375-7384, 2012.